


Semi-Automated Modular Modeling of Buildings for Model Predictive Control

Conference Paper**Author(s):**

Sturzenegger, David; Gyalistras, Dimitrios; Morari, Manfred; [Smith, Roy](#) 

Publication date:

2012-11

Permanent link:

<https://doi.org/10.3929/ethz-b-000060559>

Rights / license:

[In Copyright - Non-Commercial Use Permitted](#)

Originally published in:

<https://doi.org/10.1145/2422531.2422550>

Semi-Automated Modular Modeling of Buildings for Model Predictive Control

David Sturzenegger

Dimitrios Gyalistras

Manfred Morari

Roy S. Smith

ETH Zurich, Switzerland
Automatic Control Laboratory
www.control.ee.ethz.ch

{sturzenegger,gyalistras,morari,rsmith}@control.ee.ethz.ch

Abstract

A promising alternative to standard control strategies for heating, ventilation, air conditioning and blinds positioning of buildings is Model Predictive Control (MPC). Key to MPC is having a sufficiently simple (preferably linear) model of the building's thermal dynamics.

In this paper we propose and test a general approach to derive MPC compatible models consisting of the following steps: First, we use standard geometry and construction data to derive in an automated way a physical first-principles based linear model of the building's thermal dynamics. This describes the evolution of room, wall, floor and ceiling temperatures on a per zone level as a function of *external heat fluxes* (e.g., solar gains, heating/cooling system heat fluxes etc.). Second, we model the external heat fluxes as linear functions of control inputs and predictable disturbances. Third, we tune a limited number of physically meaningful parameters. Finally, we use model reduction to derive a low-order model that is suitable for MPC.

The full-scale and low-order models were tuned with and compared to a validated EnergyPlus building simulation software model. The approach was successfully applied to the modeling of a representative Swiss office building. The proposed modular approach flexibly supports stepwise model refinements and integration of models for the building's technical subsystems.

Categories and Subject Descriptors

I.6.4 [Simulation and Modeling]: Model Validation and Analysis

General Terms

Algorithms

Keywords

Building modeling; Model predictive control

1 Introduction

Model predictive control uses a model of the building together with predictions of relevant disturbances over a given prediction horizon to define an optimization problem for maintaining thermal comfort for the occupants while minimizing some objective (e.g. energy use or monetary cost). See [9] for a comprehensive description of MPC. In contrast to most conventional building control approaches, MPC makes it possible to integrate all available actuators and their interactions as well as predictions of weather, internal gains and electricity prices into a coherent, mathematically founded control framework which can handle constraints on inputs and room temperatures.

One proposed application of MPC to building control is in a centralized control architecture [2], [4], [12]. Here we focus on this approach for office buildings which has the advantages that the control system is typically already organized in a centralized way and that the computational constraints are not restrictive. As a part of the OptiControl¹ project, we performed a large-scale simulation study that suggested significant savings potentials of MPC when compared to industry standard control [2],[6]. In a second project phase, we have implemented a centralized MPC controlling the heating, ventilation, air conditioning/cooling (HVAC) and blinds positioning of a fully operated Swiss office building (see Figure 1(a)). We present here a general approach for deriving MPC applicable multi-zone building models and apply it to the specific architecture of the target building.

The challenge in building modeling for MPC consists in having a sufficiently detailed and precise but—for the resulting optimization problem to be tractable also for reasonably large problems—linear model of the building's thermal dynamics².

In building control literature, modeling approaches for MPC vary in the level of detail and in the extent to which they rely on identification from experiments or simulations. In [8]

¹www.opticontrol.ethz.ch (last accessed Aug 1, 2012)

²For certain building systems it may be necessary to use bilinear models, see comment in Section 3.2. In that case suboptimal solution techniques have to be employed.

the authors identified a multi-zone office building model suitable for control using black-box subspace identification from EnergyPlus³ (EP) building simulation software simulations, while the authors of [12] used a four state grey-box model with experimentally identified parameters to model two reference rooms for the heating of an office building. The approaches require either a detailed EP model or experimental data to fit the model *before* they can be applied. While this may very well be acceptable for the tasks at hand, in the case of industry application of MPC in office buildings it is unrealistic to assume that this experimental data or a detailed EP model is available beforehand. This holds especially if one wants to use more detailed (multi-zone) models which are desirable for the integrated control of office buildings' HVAC and blinds systems. Moreover, the modeling should require as little effort as possible for the approach to be attractive for practical application.

The presented method aims in this direction. We propose a semi-automated procedure that is mainly based on physical modeling using basic construction data together with a regression model for computing transmitted solar radiation.

2 MPC Model Requirements and Target Building

For use in MPC we are interested in a linear model of the form,

$$x(k+1) = Ax(k) + B_u u(k) + B_v v(k) \quad (1a)$$

$$y(k) = Cx(k) + D_u u(k) + D_v v(k), \quad (1b)$$

where $x(k), u(k), v(k), y(k)$ denote the states, the control inputs (heating/cooling etc.), the predicted disturbances (internal gains, ambient temperature, solar radiation) and the control outputs ((possibly averaged) zone temperatures) at time k , respectively. Model (1a)-(1b) is then used to predict the control outputs as a function of the current state, the control input trajectory and the predicted disturbance trajectory over a given prediction horizon. In theory, the prediction horizon should be as long as possible to ensure a good control performance. In practice however, this benefit diminishes with increasing horizon length due to deterioration of the model's and the weather forecast's prediction quality. Moreover, computational restrictions limit the achievable horizon length. Nevertheless, it is beneficial to have a horizon of at least 60h for the MPC to "see", on Friday evening, the Monday morning comfort constraints to enable the planning of the HVAC/blinds strategy during the weekend. These considerations lead us to choosing a horizon of 72h over which we compare our linear model to the detailed EP model.

For the resulting optimization problem to be convex, the actuation constraints must be convex. We use polytopic constraints having the general form

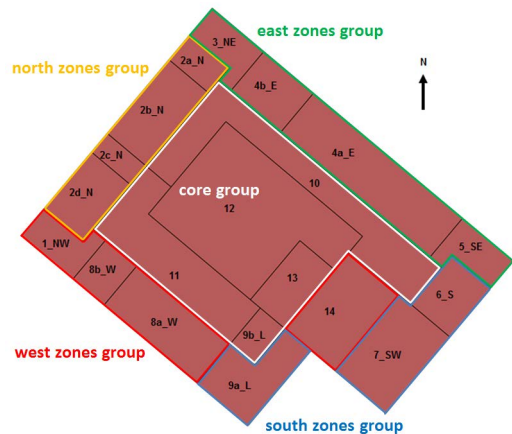
$$F(k)x(k) + G_u(k)u(k) + G_v(k)v(k) \leq g(k), \quad (2)$$

with (potentially time-varying) matrices F, G_u, G_v and a vector g of appropriate sizes.

The target building is a medium sized, representative office building located in Basel, Switzerland. The floorplan of



(a) View of the target building from south.



(b) Floorplan of the second floor considered for MPC modeling. Zone groups of which the averaged room temperatures are considered as outputs in the reduced order model are indicated.

Figure 1. Target building. Fully operated, conditioned floor area 6000m², located in Basel, Switzerland.

the second floor is shown in Figure 1(b). The HVAC system consists of the following components. First, the thermally activated building system (TABS), which are pipes buried in the concrete slabs of the floors carrying hot/cold water for energy efficient preheating/precooling. See [11] for a comprehensive treatment of TABS. Second, an air handling unit (AHU) that includes a return air heat recovery system, an evaporative cooler and a heater. Third, the blinds which are also controlled centrally. The cold water for the TABS is generated using a cooling tower (a heat exchanger to the ambient air) while the hot water for the TABS and the AHU heater is generated using a gas boiler.

In order to be able to predict lateral temperature variations within the building, we chose to model the entire second floor. The floors and ceilings were modeled to have adiabatic boundary conditions.

3 Building Modeling Method for MPC

In the following sections we describe the four steps of the proposed modeling method. In Section 3.1 we use standard geometry and construction data to derive in an auto-

³<http://apps1.eere.energy.gov/buildings/energyplus/> (last accessed Aug 1, 2012)

mated way a physical first-principles based linear model of the building's thermal dynamics⁴ as a function of external heat fluxes $q(x(t), u(t), v(t))$

$$\dot{x}(t) = A_t x(t) + B_t q(x(t), u(t), v(t)). \quad (3)$$

In Section 3.2 we describe these heat fluxes as functions of control inputs and predictable disturbances in the following form

$$q(x(t), u(t), v(t)) = A_q x(t) + B_{q,u} u(t) + B_{q,v} v(t), \quad (4)$$

with (if applicable) their corresponding actuation constraints. Model (3) is combined with (4) and subsequently discretized. In Section 3.3 we list the model's tuning parameters and motivate their choice. Finally in Section 3.4, we define control outputs and use a standard model reduction technique to obtain a MPC compatible model.

3.1 Step 1: Automated Thermal Dynamics Model Generation

In this section we outline the generation of model (3) from basic construction data. In this context we use "building element" to describe walls, floors, ceilings and internal mass. In the literature on simplified building modeling, the main approach is to model zones and building elements linearly using lumped states that describe their temperature, and calculate resistances and heat capacities that define the heat exchange between them. Due to the obvious analogy to electrical circuits, this is also called *resistance-capacitance* (RC) modeling. See for instance [13] or [14] for grey-box building models or [1], [5], [3] for white-box models relying solely on physical first-principles. The white-box building modeling literature mainly uses a single state to model a zone's air temperature, but differs in the number of states describing the temperatures within a building element. Since model reduction is part of our approach, the initial number of states modeling a building element is not as critical in terms of final model complexity. We therefore use the well validated approach of [3] which uses one state per building element layer to obtain a single-zone model. In this paper we connect multiple of these models to build a complete floor model. Figure 2 shows the RC schematic of a single zone i including a floor, a ceiling, an exterior wall and an interior wall branch as well as capacitances for the zone air temperature and the internal mass. For simplicity, only one interior and exterior wall branch and a fixed number of three states (capacitances) per building element are shown (there may be more or less). Table 1 lists all indicated external heat fluxes, the node at which they apply and the physical heat flux they represent. Detailed descriptions of the external heat fluxes are given in Section 3.2. Note that the illustrated zone is adiabatic except for the branch to the adjacent zone and the external heat fluxes and hence the overall thermal model is adiabatic except for the external heat fluxes.

Algorithm 1 constructs the building's thermal model (3). As input the following objects are needed:

1. A list of zones containing for each zone its air volume;

⁴We use the subscript "t" to denote matrices of the thermal dynamics model (e.g. A_t) and subscript "q" for matrices of the external heat flux models

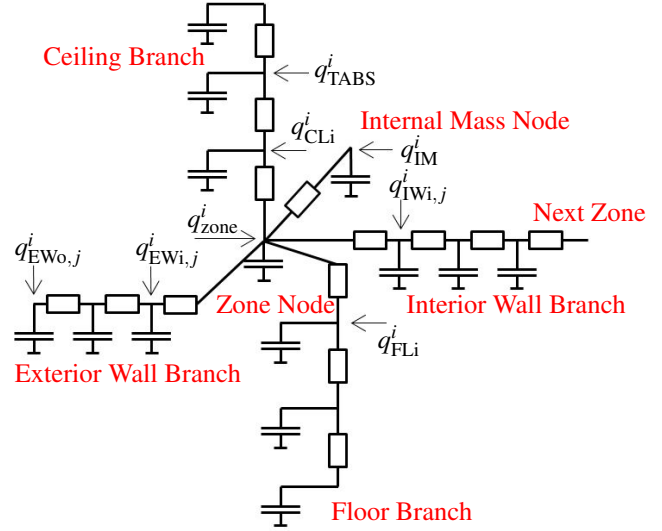


Figure 2. RC network for zone i . Capacitances represent states, resistances the thermal resistances and q external heat fluxes.

Table 1. External heat flux symbols and descriptions for zone i .

Symbol	Node of application	Physical heat flux
q_{zone}^i	zone	internal gains, window heat fluxes
$q_{EWo,j}^i$	outermost of ext. wall j	solar radiation and convection
q_{TABS}^i	TABS layer	TABS gains
q_{FLi}^i	innermost of floor	solar radiation
q_{CLi}^i	innermost of ceiling	solar radiation
$q_{EWi,j}^i$	innermost of ext. wall j	solar radiation
q_{IWj}^i	innermost of int. wall j	solar radiation
q_{IM}^i	internal mass	solar radiation

2. A list of all building elements containing for each building element its construction type, area and identifiers of the adjacent zones;
3. A list of construction types containing for each construction type all layers with corresponding thicknesses, heat capacities and thermal resistances.

The listing of Algorithm 1 contains the following functions. The function `get_element_model(.)` generates the building element's system matrix \bar{A}_{el} , its (diagonal) capacitance matrix Z_{el} as well as the (possibly empty) external heat flux input matrix B_{el} according to the construction type and area specified in the building element. The function `connect_element_to_adjacent_zones(.)` then adds appropriate entries (inverse heat transfer resistances) in the \bar{A} matrix to model the heat transfer between the building element and its adjacent zones. These resistances contain convective coefficients which we consider as tuning parameters (see Section 3.3). Refer to [3] for a more detailed description of the approach we use to model building elements.

Data: 'list of zones', 'list of building elements', 'list of construction types'

Result: Thermal model of the form (3)

Initialize empty capacitance matrix Z , empty resistance matrix \bar{A} , empty external heat flux matrix \bar{B} ;

for all zones **do**

compute 'zone capacitance';
 $\bar{A} = \text{bdg}^5(\bar{A}, 0)$; $\bar{B} = \text{bdg}(\bar{B}, 1)$;
 $Z = \text{bdg}(Z, \text{'zone capacitance'})$;

end

for all building elements **do**

$[\bar{A}_{el}, Z_{el}, B_{el}] = \text{get_element_model}(\text{'building element'}, \text{'list of construction types'})$;
 $\bar{A} = \text{bdg}(\bar{A}, \bar{A}_{el})$; $\bar{B} = \text{bdg}(\bar{B}, B_{el})$; $Z = \text{bdg}(Z, Z_{el})$;
 $\bar{A} = \text{connect_element_to_adjacent_zones}(\bar{A}, \text{'building element'})$;

end

$A_t = Z^{-1}\bar{A}$;

$B_t = Z^{-1}\bar{B}$;

Algorithm 1: Automated generation of the thermal dynamics model.

3.2 Step 2: Adding External Heat Flux Models

External heat fluxes describe all heat fluxes into the building and to its hull that are not direct heat exchanges among building elements and zones. For different building cases, the external heat flux models may have similar forms (e.g. convective losses to the environment, or internal gains) but can also vary substantially on a case-to-case basis due to the differences in the type of HVAC subsystems.

The approach proposed in this paper allows for a modular addition of these subsystems to the thermal dynamics model. Due to the large variety, it is not possible to give models for all existing HVAC systems, but we limit ourselves to describing a subset of the external heat flux models we have developed for the target building. These models include the convective heat flux and solar gains to the building hull, convective and solar radiation gains through the windows as a function of blind position, internal gains due to occupants and appliances as well as heating/cooling gains from the TABS. We do not show models of the AHU or air infiltration. For a detailed modeling of the target building's AHU refer to [10] and for models of further HVAC subsystems refer to [3].

Note that even though we require a linear form (4) it is possible (and in the case of ventilation systems typically necessary) to relax this restriction to models containing bilinear terms in inputs and disturbances ($u_i \cdot v_j$) and in inputs and states ($u_i \cdot x_j$). Since this results in a (mildly) nonlinear optimization problem, it makes the use of suboptimal solution techniques such as sequential linear programming necessary. It was shown in [2] that this approach gives reasonable results.

For the windows and building hull models the diffuse and

$$s_{\text{bdg}}(a, b) := \begin{bmatrix} a & 0 \\ 0 & b \end{bmatrix}.$$

direct components of the solar radiation on the different parts of the facade have to be computed from the global solar radiation on a horizontal surface. We use the Perez direct/diffuse split model [7] and basic trigonometry to compute the facade incident radiation.

In the following we will consider q_{zone}^i in two parts, an internal gains and a window heat flux, i.e.

$$q_{\text{zone}}^i = q_{\text{zone,IG}}^i + q_{\text{zone,win}}^i.$$

3.2.1 Internal gains

Internal gains due to occupants, lighting and appliances are considered as simple convective heat sources and denoted by v_{IG} in Watts per squaremeter floor area (for simplicity we assumed the same value for all zones), i.e. for zone i with floor area a^i we have,

$$q_{\text{zone,IG}}^i = a^i v_{\text{IG}}(t).$$

3.2.2 Building hull

Consider exterior wall j of zone i with area $a_{\text{EW},j}^i$. The convective heat flux is modeled to be proportional to the temperature difference between the outermost layer of exterior wall j , i.e. $x_{\text{EW},j}^i$, and the ambient air temperature v_{Ta} . The solar radiation heat gains are considered to be the product of the global radiation incident onto the exterior wall, $v_{\text{solGlobEW},j}^i$ (in Watts per squaremeter wall area), and an absorption coefficient, γ_{absorp} . The latter coefficient as well as the convective coefficient, α_{EW} , are tuning parameters of our model (see Section 3.3). We then have

$$q_{\text{EW},j}^i = a_{\text{EW},j}^i \alpha_{\text{EW}} (v_{\text{Ta}}(t) - x_{\text{EW},j}^i(t)) + \gamma_{\text{absorp}} v_{\text{solGlobEW},j}^i(t).$$

For simplicity we will in the following approximate $v_{\text{solGlobEW},j}^i$ by the average global radiation incident onto the corresponding facades, i.e. by the appropriate element in $\{v_{\text{solGlobFac},\text{N}}, v_{\text{solGlobFac},\text{E}}, v_{\text{solGlobFac},\text{W}}, v_{\text{solGlobFac},\text{S}}\}$.

3.2.3 TABS

The heat flux to the TABS slab node of zone i is modeled to be a floor area proportional fraction of the total TABS heat fluxes which are denoted by $u_{\text{TABS,h}}$ and $u_{\text{TABS,c}}$ (the latter being positive if cooling is active). Hence, using $a_{\text{TABS,tot}}$ as the total area of all zones equipped with TABS and a^i as the floor area of zone i we have,

$$q_{\text{TABS},i} = \frac{a^i}{a_{\text{TABS,tot}}} (u_{\text{TABS,h}}(t) - u_{\text{TABS,c}}(t)).$$

The TABS heating constraint is approximated by the maximum power supplyable by the boiler $Q_{\text{TABS,h,max}}$. Since the TABS cooling circuit is fed by a cooling tower (essentially a heat exchanger to the ambient air), the maximum available TABS cooling power is a function of v_{Ta} and the TABS slab temperatures. In [11] a formula was derived to calculate an equivalent resistance R_t on the basis of the TABS construction details. The maximum heat flux is modeled as

$$Q_{\text{TABS,c,max}}(x(t), v_{\text{Ta}}(t)) = \frac{a_{\text{TABS,tot}}}{R_t} (v_{\text{Ta}}(t) - T_{\text{avgTABSslab}}(x(t))),$$

where $T_{\text{avgTABSslab}}$ is the area weighted average TABS slab temperature which is a linear function of x . The constraints

can then be written as

$$\begin{aligned} 0 &\leq u_{\text{TABS,h}}(t) \leq Q_{\text{TABS,h,max}} \\ 0 &\leq u_{\text{TABS,c}}(t) \leq Q_{\text{TABS,c,max}}(x(t), v_{Ta}(t)). \end{aligned}$$

3.2.4 Window heat fluxes

Unsurprisingly, the window modeling turned out to be crucial for a good model performance. We denote direct and diffuse radiations onto window j of zone i by $v_{\text{solDirWin},j}^i$ and $v_{\text{solDiffWin},j}^i$, respectively. We consider the heat flux through the windows in three parts; a radiation part which we model to directly act on the innermost layers of the building elements directly in contact with the zone's air (see Figure 2), a heat flux due to conduction through the window and an additional heat flux due to absorption of solar radiation and subsequent heating up of the window. The first part constitutes the heat fluxes $q_{\text{FL},i}^j$, $q_{\text{CL},i}^j$, $q_{\text{EW},i,j}^j$, $q_{\text{IW},i,j}^j$ and q_{IM}^i while the latter two are reflected in $q_{\text{zone,win}}^i$.

We model the blinds control input u_{bl}^i of zone i as a controllable heat flux with the minimum constraint being the heat flux with blinds set to maximum allowed shading position while the maximum heat flux is given by the heat flux with blinds set to open position. The conductive heat flux through windows is modeled to be proportional to the difference of the ambient air temperature and the zone temperature $x_{\text{zone},i}$. We model the additional heat gains due to absorption of solar radiation by the product $\gamma_{\text{winSolAbs}} u_{bl}^i$. Using $a_{\text{win,tot}}^i$ as the total window area of zone i and U_{win} as the windows' heat transmission factor we get for the window heat flux acting on the zone node

$$q_{\text{zone,win}}^i = U_{\text{win}} a_{\text{win,tot}}^i (v_{Ta}(t) - x_{\text{zone}}^i(t)) + \gamma_{\text{winSolAbs}} u_{bl}^i(t).$$

In this, $\gamma_{\text{winSolAbs}}$ and U_{win} are tuning parameters of our model (see Section 3.3). For the heat flux on the building element nodes with total area $a_{\text{BE,tot}}^i$ (here shown for interior wall j with area $a_{\text{IW},j}^i$, analogously for the other building elements) we have,

$$q_{\text{IW},j}^i = \frac{a_{\text{IW},j}^i}{a_{\text{BE,tot}}^i} u_{bl}^i(t).$$

The constraints on u_{bl}^i are given by

$$\begin{aligned} Q_{bl,min}^i(v_{\text{solDirWin},j}^i(t), v_{\text{solDiffWin},j}^i(t)) &\leq u_{bl,i}(t) \\ u_{bl,i}(t) &\leq Q_{bl,max}^i(v_{\text{solDirWin},j}^i(t), v_{\text{solDiffWin},j}^i(t)). \end{aligned}$$

Computing $Q_{bl,min}^i$ and $Q_{bl,max}^i$ can be done offline. To have an as accurate model as possible without having to model detailed blinds physics, we identified from EP a regression model

$$Q_{bl,j}^i = \alpha v_{\text{solDiffWin},j}^i + \beta v_{\text{solDirWin},j}^i + \gamma (v_{\text{solDirWin},j}^i)^2 + \delta,$$

where α , β , γ are functions of the calendar month, the facade orientation and the blind position and δ is in addition a function of the hour of day. The parameters α to δ were estimated by a multivariate linear regression based on outputs $Q_{bl,j}^i$, $v_{\text{solDiffWin},j}^i$ and $v_{\text{solDirWin},j}^i$ from a year-long EP simulation.

3.2.5 Discretization

Adding the external heat flux models (4) to the thermal dynamics model (3) yields a continuous time model in $x(t), v(t), u(t)$ which we subsequently discretize at a 15 minute sampling rate.

3.3 Step 3: Model tuning

Table 2. Overview of tuning parameters.

Parameter	Description	Tuned value
α_{IW}	int. wall conv. coeff.	8.4 [W/(m ² K)]
α_{FL}	floor conv. coeff.	2.4 [W/(m ² K)]
α_{CL}	ceiling conv. coeff.	5.6 [W/(m ² K)]
α_{EW}	ext.wall conv. coeff.	12.5 [W/(m ² K)]
γ_{absorp}	building hull solar absorption factor	0.6 [-]
$\gamma_{\text{winSolAbs}}$	window additional heat gain factor	0.35 [-]
U_{win}	window heat transmission value	1.25 [W/(m ² K)]

Our model contains seven tuning parameters as listed in Table 2. The motivation for tuning the convective coefficients was to adjust the according heat fluxes for unmodeled radiation and air motion effects. The window transmission value and additional heat gain factor turned out to be needed to linearly represent the complicated window physics. The facade absorption parameter was tuned because its value was considered to be unknown.

All other parameter values (excepting the solar regression model) were computed from construction data.

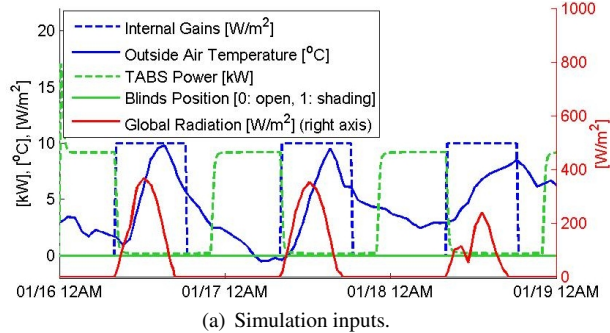
3.4 Step 4: Model reduction

To reduce the model order we first define a set of outputs we want to control. We use a Hankel norm based approach to compute a linear map $T \in \mathbb{R}^{n \times m}$, $n \ll m$ that defines a transformation $\tilde{x} = Tx$ such that the resulting low-order model has a closely matching input-output behavior.

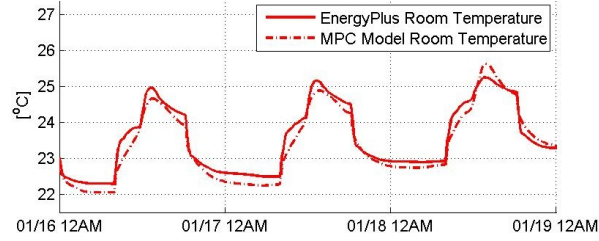
As control outputs we defined the averaged temperatures of the rooms of each of the four facades as well as the center zone, see Figure 1(b). Note that the minimum order of the model depends on the number of inputs and outputs. Hence we computed (as in the case of hull solar absorption) average solar gains per facade to lower the number of solar gains inputs to 5 (one per individually actuatable set of blinds) in order to be able to further reduce the model order. The result was a model having 5 outputs and 13 inputs including 5 for the window solar gains for each facade zone, 2 for the TABS, 4 for the irradiation on the facades, one for the ambient air temperature and one for the internal gains. The number of states was reduced from 372 to 25.

4 Application of Method and Testing

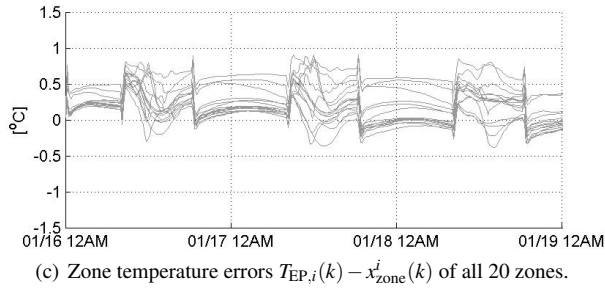
Two possibilities exist for testing a model; either the model's predictions are compared to measurements taken on a real system or they are compared to the predictions of a reference model. Clearly, the first approach allows to make a more definitive statement on the model performance since its final goal is to predict reality but the latter typically gives



(a) Simulation inputs.



(b) EP and RC model temperatures of the room with median average error $E_{mean,i}$ (see Equation (5a)).



(c) Zone temperature errors $T_{EP,i}(k) - x_{zone}^i(k)$ of all 20 zones.

Figure 3. Heating case simulation. Weather was recorded from January 16-19, 2011, in Basel, Switzerland. $E_{mean} = 0.25K$

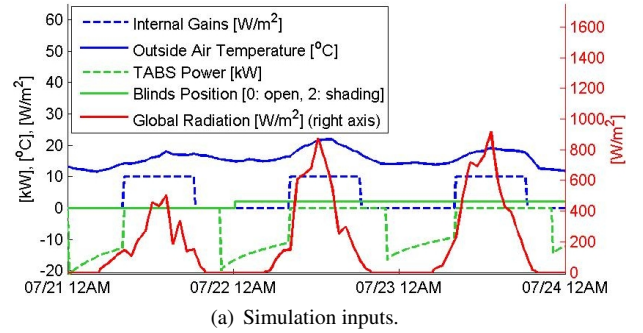
more insight into potential model discrepancies due to flexibility in setting up simulation experiments and the ability to directly access most of the relevant physical quantities. In the latter approach, the implicit assumption is that the reference model reflects reality to a sufficient degree of accuracy.

In this paper we used EP as our reference model. The EP model has been built by building simulation experts from Gruner AG, Switzerland⁶ and was partly validated with satisfying results (full validation ongoing) by comparing with measurements from the target building.

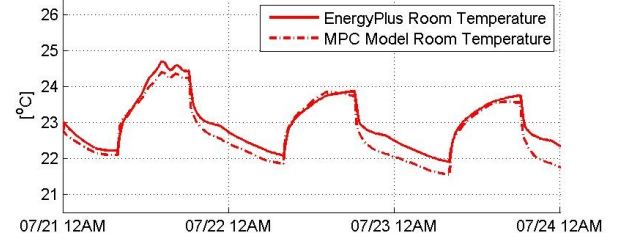
4.1 Parameter tuning

For the tuning we used two three-day simulation periods with spring and autumn conditions. The evaluation of the tuned model used winter and summer simulation periods. A grid search space method centered around physically reasonable initial values was used. The resulting set of tuned parameter values was chosen by minimizing the average zone temperature errors over both tuning periods.

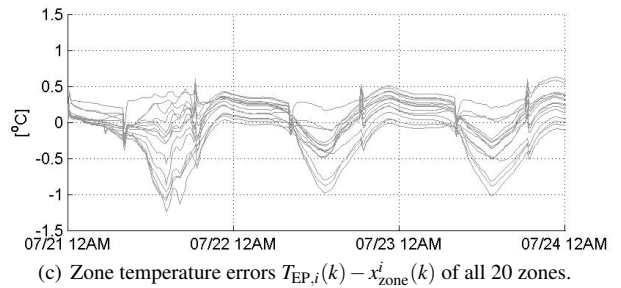
⁶www.gruner.ch/gruner/home (last accessed Aug 1, 2012)



(a) Simulation inputs.



(b) EP and RC model temperatures of the room with median average error $E_{mean,i}$ (see Equation (5a)).



(c) Zone temperature errors $T_{EP,i}(k) - x_{zone}^i(k)$ of all 20 zones.

Figure 4. Cooling case simulation. Weather was recorded from July 21-24, 2011, in Basel, Switzerland. $E_{mean} = 0.21K$

4.2 Full-scale model testing

The main evaluation of the model's predictive quality was the comparison of the full-scale model to EP, since a good full-scale model on one hand yields a good reduced order model (given a reasonable reduction) and on the other hand allows for the consistent incorporation of external heat flux models that may depend for instance on accurate single zone temperature predictions.

We first defined and ran a simulation in EP and stored the room temperature trajectories. Then we used the same inputs (weather, internal gains, heating/cooling/blinds commands) to simulate the RC model. Finally we compared the EP with the RC simulated room temperatures by computing two error measures, the mean as well as the maximum of the absolute error on a per zone basis.

$$E_{mean,i} := \frac{1}{n_k} \sum_{k=1}^{n_k} |T_{EP,i}(k) - x_{zone}^i(k)| \quad (5a)$$

$$E_{max,i} := \max_k |T_{EP,i}(k) - x_{zone}^i(k)|. \quad (5b)$$

In this, n_z , n_k denote the number of zones and simulation

time steps and $x_{\text{zone}}^i(k)$, $T_{\text{EP},i}(k)$ denote the RC model's and EP model's temperature value of zone i at time k . We also used analogous values on a per floor basis, i.e.,

$$E_{\text{mean}} := \frac{1}{n_z} \sum_{i=1}^{n_z} E_{\text{mean},i} \quad (6a)$$

$$E_{\text{max}} := \max_i E_{\text{max},i}. \quad (6b)$$

We compared our model in a heating and a cooling case. The building was in both cases initialized to a constant temperature of 23°C in order to have identical initial conditions.

For both simulations we used real weather data recorded in Basel in 2011. In Subfigure a) of Figures 3 and 4, we show the inputs to the simulations, in b) EP and RC model temperatures of the median $E_{\text{mean},i}$ zone and in c) the errors $T_{\text{EP},i}(k) - x_{\text{zone}}^i(k)$ of all 20 zones.

Figure 3 shows the heating case simulation starting on January 16. The ambient air temperature varied between -1°C and 10°C , internal gains were set to $10\text{W}/\text{m}^2$ during office hours and a periodic TABS heating signal of 9kW was applied. The blinds were open all the time. In Figure 3(b) it can be seen that in this zone $E_{\text{mean},i} \approx 0.25\text{K}$, $E_{\text{max},i} \approx 0.5\text{K}$ with a temperature trajectory peak-to-peak value of 3K . Figure 3(c) finally shows the errors of all zones which range from -0.4K to 0.9K with $E_{\text{mean}} = 0.25\text{K}$.

Figure 4 shows the cooling case simulation starting on July 21. The ambient air temperature varied between 10 and 22°C , internal gains were set to the same schedule as in the heating case and a periodic TABS cooling signal was applied. After the first day, the blinds were set to a shading position. In Figure 4(b) it can be seen that in this zone $E_{\text{mean},i} \approx 0.2\text{K}$, $E_{\text{max},i} \approx 0.5\text{K}$ with a peak-to-peak value of 2.7K . Figure 4(c) shows the errors of all zones which range from -1.2K to 0.7K with $E_{\text{mean}} = 0.21\text{K}$. The largest absolute values of the error were observed during the first day when blinds were open.

4.3 Low-order model testing

We show in Figure 5 for the cooling case the difference between the weighted average zone temperatures as computed from EP and the same quantities for the reduced order model (see Section 3.4). Unsurprisingly, the errors have a similar profile as in Figure 4(c). Nevertheless E_{max} was reduced by the averaging process from 1.2K to 1K , even though the number of controllable heat fluxes had been reduced by taking average values.

4.4 Sensitivity study

Figure 6 shows the sensitivities of the full-scale model with respect to changes in the tuning parameters. For all parameters shown in Table 2 we calculated relative changes in two error metrics $(E_{\text{mean,Jan}} + E_{\text{mean,July}})/2$ and $\max(E_{\text{mean,Jan}}, E_{\text{mean,July}})$ denoted in Figure 6 as "mean error" and "max error" to $\pm 20\%$ changes of each individual parameter (the others were fixed at the nominal value as given in Table 2).

We found that only three (α_{CL} , $\gamma_{\text{winSolAbs}}$, U_{win}) of the seven parameters had a significant impact on the model performance, the others' influences were within $\pm 5\%$ of the nominal model's error.

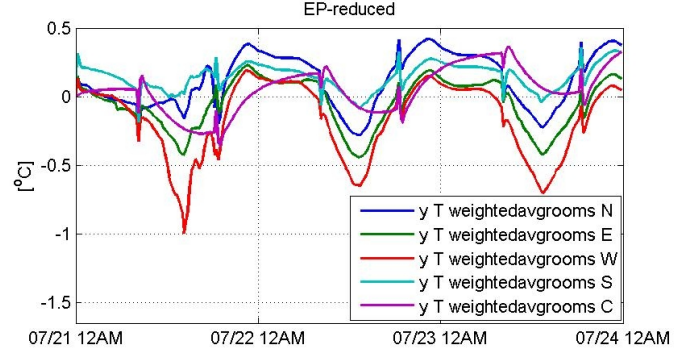


Figure 5. Output errors of reduced model (EP value - reduced model value). Outputs are averaged room temperatures. For the grouped zones see Figure 1(b).

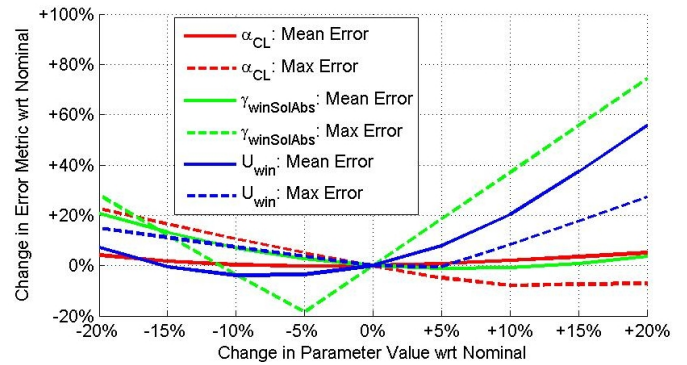


Figure 6. Relative changes of mean and maximum error (as defined in Section 4.4) with respect to changes in the three most sensitive parameters. Nominal mean and maximum error were 0.23K and 1.2K , respectively. Nominal parameter values shown in Table 2.

5 Discussion

The results showed that the full scale model is capable of predicting individual room temperatures in a cooling and a heating case with a maximum error of 1.2K and a much smaller average error of around 0.25K when compared to EnergyPlus simulations. The maximum error is not negligible compared to typical comfort ranges in building control and this can have some impact on the MPC's control decisions due to its constraint avoidance. However, because of the large discrepancy between average and maximum error, it can be expected that by defining control outputs as averages of thermally similar zones (e.g. on the same facade) the maximum error can be reduced while keeping enough model detail to predict facade-wise temperature variations. In Section 4.3 this effect has been shown for the summer case where the maximum error was reduced from 1.2K to 1K . An MPC using a model generated by an earlier, less elaborated, approach showed reasonable control actions throughout its first phase of application on the target building from April to August 2012. We expect that using better models generated based on the present work will further improve its performance.

Development of our simplified model required availability of a detailed EnergyPlus model for (i) parameter tuning, and (ii) identifying a regression model for computing solar heat gains as a function of the incident solar radiation and the blinds position. If an EnergyPlus model of a given building is available, it certainly can and should be used to improve the MPC model as was done here. If however no detailed building model is at hand (which is not unlikely in a practical application), points (i) and (ii) need to be addressed. We believe that the EnergyPlus dependence can be dropped with reasonable effort: (i), the tuning parameters have a physical meaning such that reasonable initial values can be chosen and refined by measurements during online operation. As for (ii), it is unlikely that the currently used detailed regression model could be identified on an operating building, since solar fluxes are typically only indirectly measured via room temperatures. However, it may be possible to obtain simpler, yet for our purposes sufficiently accurate, models from measured data. These points will be addressed in future work.

Our choice was to build a detailed model from physical first-principles using basic construction data. Some alternatives to this choice exist, such as using a grey-box modeling approach and identifying model parameters from measurements, or identifying black-box models from simulations. However, we believe that our approach is better suited for modeling office buildings for MPC because it allows for physical interpretation of input-output relationships and because it can be easily adapted to changing zone geometries, HVAC systems etc. In contrast, black-box model identification from detailed simulations requires re-identification from scratch and updated detailed models for varying building cases. In grey-box identification methods a good initial model structure is not always easily found. Moreover, in both mentioned alternative approaches either measurement data or a detailed model are absolutely necessary *before* the corresponding controller can be applied, while—if points (i) and (ii) were addressed—the presented approach could be used without any prior knowledge except for the construction data.

Even though the EnergyPlus model has already partly been validated against measured data, a definitive statement about the RC model's predictive quality can only be made by direct comparison with measurements. However, the comparison of the RC model to EnergyPlus gave valuable insights which could not have been gained by comparing to measured data because of restrictions in viable experiments. The RC model's validation against measurements is planned to be addressed in future work.

6 Conclusions

The proposed approach combines the application of basic physical laws with building-specific data into a systematic modeling procedure for generating MPC applicable models. External heat flux models related to disturbances and technical systems can be readily included in a modular way. The effort for the formulation of appropriate submodels leading to an overall model suitable for MPC varies strongly on a case-by-case basis. Tuning of the model and a part of the solar heat flux calculations currently require the availability

of a detailed building model.

Temperature errors of the resulting model averaged over all zones and time steps of two (heating case, cooling case) three-day simulations were found to be less than 0.25K when compared to a detailed building simulation software. The resulting full-scale linear model enables the realistic simulation of a building's thermal dynamics at the level of individual zones. Defining a limited set of control outputs and reducing the model order allows for application of the resulting model in MPC.

7 Acknowledgements

We would like to thank Carina Sagerschnig (Gruner AG, Switzerland) and Markus Gwerder (Siemens Switzerland Ltd.⁷) for their support within the OptiControl project and with EnergyPlus. This work was financially supported by Siemens Switzerland Ltd. and swisselectric research⁸.

8 References

- [1] M. Gouda, S. Danaher, and C. Underwood. Building thermal model reduction using nonlinear constrained optimization. *Building and Environment*, 37(12):1255 – 1265, 2002.
- [2] D. Gyalistras and M. G. (Eds.). Use of weather and occupancy forecasts for optimal building climate control (OptiControl): Two years progress report. Technical report, ETH Zurich and Siemens Building Technologies Division, Siemens Switzerland Ltd., Zug, Switzerland, 2009.
- [3] B. Lehmann, K. Wirth, S. Carl, V. Dorer, T. Frank, and M. Gwerder. Modeling of buildings and building systems. Technical report, 2009. in [2].
- [4] Y. Ma, F. Borrelli, B. Hency, B. Coffey, S. Bengea, and P. Haves. Model predictive control for the operation of building cooling systems. *Control Systems Technology, IEEE Transactions on*, 20(3):796 –803, may 2012.
- [5] G. Masy. *Definition and validation of a simplified multizone dynamic building model connected to heating system and HVAC unit*. PhD thesis, Université de Liege, 2008.
- [6] F. Oldewurtel, A. Parisio, C. Jones, D. Gyalistras, M. Gwerder, V. Stauch, B. Lehmann, and M. Morari. Use of model predictive control and weather forecasts for energy efficient building climate control. *Energy and Buildings*, 45:15–27, 2012.
- [7] R. Perez, P. Ineichen, E. Maxwell, R. Seals, and A. Zelenka. Dynamic global-to-direct conversion models. *ASHREA transactions*, pages 254 – 369, 1992.
- [8] S. Prívvara, Z. Vana, D. Gyalistras, J. Cigler, C. Sagerschnig, M. Morari, and L. Ferkl. Modeling and identification of a large multi-zone office building. In *Control Applications (CCA), 2011 IEEE International Conference on*, pages 55 –60, sept. 2011.
- [9] J. Rawlings and D. Mayne. *Model Predictive Control: Theory and Design*. Nob Hill Publishing, 2009.
- [10] D. Sturzenegger. Bilinear modeling for model predictive control of an air handling unit. Technical report, ETH Zurich, 2012. www.control.ee.ethz.ch.
- [11] J. Toedtli, M. Gwerder, B. Lehmann, and F. Renggli. *TABS Control faktor*, 2009.
- [12] J. Široký, F. Oldewurtel, J. Cigler, and S. Prívvara. Experimental analysis of model predictive control for an energy efficient building heating system. *Applied Energy*, 88(9):3079 – 3087, 2011.
- [13] S. Wang and X. Xu. Parameter estimation of internal thermal mass of building dynamic models using genetic algorithm. *Energy Conversion and Management*, 47(1314):1927 – 1941, 2006.
- [14] R. Yao, N. Baker, and M. McEvoy. A simplified thermal resistance network model for building thermal simulation. In *eSim, Montreal, Canada (2000)*, pages 135–140, 2000.

⁷www.siemens.ch (last accessed Aug 1, 2012)

⁸www.swisselectric-research.ch/ (last accessed Aug 1, 2012)